University of Bath

Geotechnical installation design of suction buckets in non-cohesive soils: a reliability-based approach

Joost Remmers[a,b,c], Cormac Reale[a,d], Federico Pisanò[a], Sylvie Raymackers[b], Kenneth G. Gavin[a]

[a]*Section of Geo-Engineering, Delft University of Technology, The Netherlands.*
[b]*GeoSea (DEME Group), Haven 1025, Scheldedijk 30, 2070 Zwijndrecht, Belgium*
[c]*Temporary Works Design, Marconistraat 16, 3029 AK, Rotterdam, The Netherlands*
[d]*Department of Architecture & Civil Engineering, University of Bath, United Kingdom*

Abstract

This study presents a probabilistic analyses of suction bucket installation in cohesionless soils. The spatial variability of soil properties is quantified using a representative survey dataset from practice. Vertical random field modelling is used to model cone resistance variability and probability density functions are fitted using drained parameter estimates. Conventional installation analysis methods are adapted for layered soil deposits. The effect of varying permeability is included through the incorporation of a finite element seepage model. Parametric uncertainties are considered through a Monte Carlo analysis and the results are interrogated through a variety of feasibility and sensitivity studies. Performing such an analysis allows a designer to gain insights into governing failure mechanisms and objectively quantify the impact of uncertainty regarding parameter estimates.

Keywords: Suction buckets, Geotechnical installation, Uncertainty analysis, Spatial variability

1. Introduction

Offshore wind developments are moving to deeper waters, as suitable near-shore sites become increasingly difficult to find. In addition environmental regulations regarding installation noise are becoming more strict. Suction buckets provide a quieter, rapid installation alternative to piled foundations and are comparatively simple to decommission [1]. They can be used as a foundation or anchoring system for either bottom-founded or floating wind turbines [2]. According to the latest WindEurope report [3], suction buckets comprise a very small percentage of offshore wind foundations in European developments at this moment, with piling still the preferred option. Unfortunately, this means there is little practical guidance or precedence on suction bucket installation. Assessment of the feasibility of suction bucket installation is hindered as a consequence.

A suction bucket foundation consists of an upside down bucket which is installed through the generation of reduced pressure within the buckets enclosed area [4]. Characterising in-situ soil properties and how they vary across a site is of critical importance when assessing the feasibility of suction buckets [1]. Parameter variability is of particular importance when assessing in-situ soil strength and permeability. Unfortunately, permeability is notoriously difficult to measure accurately but of paramount importance to the successful installation of suction buckets [5]. This paper provides insight into the impact of uncertainties on the installation design.

Engineers have a number of competing strategies for considering uncertainty: 1). *ignoring it altogether* - a surprisingly common but dangerous practice, 2). *being conservative* - a practice which generally results in a safe but overly expensive design. The primary drawback being that without explicitly considering variability it is impossible to determine how conservative one is being. 3). *the observational method*, which involves changing the design during construction or operation to accommodate observed behaviour and correct for it. While this approach is quite successful in its own right it has a number of drawbacks, mainly changing costs and construction times. 4). *Quantify uncertainties*, using reliability-based design methods [6]. While the first three can only give an impression of certainty the latter can explicitly account for uncertainties and give a true measure of conservatism [7]. Reliability-based design methods were originally developed to model low rate of occurrence and high risk problems such as those encountered in nuclear design [6]. To accurately apply these methods in the geotechnical domain, realistic descriptions of measurement errors, model errors and the spatial variability of soil properties are required [8]. Unfortunately, these are difficult to obtain due to the limited availability of measurements and the large inherent uncertainty in geotechnical parameter estimation approaches [9]. Nevertheless, these methods have been successfully applied in the fields of levee design, slope stability, bearing- and lateral pile capacity among others [8], [10], [11], [12], [13]. To date however, there are few practical examples of reliability being applied to quantify uncertainty in the installation of offshore foundations [14]. Reliability based approaches are ideal for the consideration of installation studies given the costs and risks involved.

This study demonstrates how reliability methods can be used to investigate the impact material uncertainty has on the installation of suction buckets in cohesionless soils. Qualitative reliability analyses, that focus on events and failure mechanisms which could arise during installation, are performed. Two design methods for suction bucket installation are analysed and adapted for layered soils with varying permeabilities. Spatial variability of parameters is objectively quantified in order to apply reliability-based design to suction bucket installation design methods. A representative geotechnical survey from an offshore wind farm is used to obtain the variability estimates. Quantified parametric uncertainties are implemented in the adapted design methods using a Monte Carlo simulation. The results are used to assess the impact of parametric variability in a series of feasibility and sensitivity studies.

2. Analysing suction bucket installation

Before performing a quantitative reliability assessment, qualitative reliability methods are considered to account for and relate failure events (that are not directly accounted for) to traditional design methods. Figure 2 displays the followed procedure during the analysis.

2.1. Overview of suction bucket installation

The installation of suction buckets has a number of phases. In the initial phase the suction bucket penetrates into the seabed under its own weight. Before breaching further into the seabed the bucket must first penetrate through the scour protection layer previously placed at the site [15], [16]. When the soil resistance equalises with the submerged weight on the bucket,
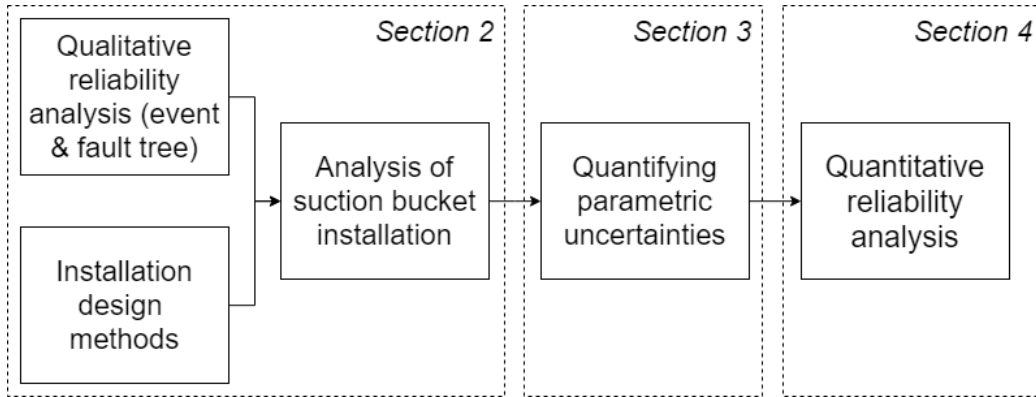
4

Figure 1: Methods (with Sections) forming the reliability analysis performed in this study

water is pumped out of the bucket cavity. This generates a pressure differential (s) within the bucket cavity relative to the surrounding water pressure (Figure 5). This under pressure results in a net downward driving force (in addition to the self weight) and causes seepage flow into the bucket as water pressure attempts to equilibrate. The seepage flow reduces the soil's effective stress profile along the inside and under the bottom annulus of the bucket. Thereby reducing the soils resistance to suction bucket installation [4], [17]. Installation is considered to be successful if the bucket reaches its target depth without refusal or structural damage.

Between placing the suction bucket on the filter layer and reaching target depth, different events can occur which can lead to installation failure. Some of the phenomena causing failure can be mitigated through the application of contingency measures. Prior to examining quantitative design methods, the whole installation process is qualitatively inspected by means of event tree (subsection 2.2) and fault tree analyses (subsection 2.3).

5

2.2. Event tree analysis

An event tree is a method of mapping all possible scenarios between the initiating event (placement of the bucket on the filter layer) and all possible outcomes (installation success/failure) using Boolean logic to determine subsequent consequences [6], [18]. An objective analysis of the impact of hazards and the effectiveness of contingency measures is possible with an event tree, provided that all probabilities inside the tree are unconditional and mutually exclusive [7]. Figure 2 presents a general event tree of suction bucket installation.
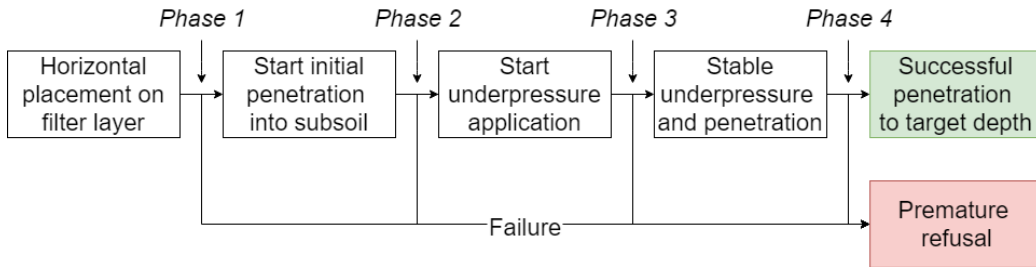

Figure 2: General event tree for geotechnical installation of suction buckets

Specific causes of premature refusal can be (partially) mitigated by the application of contingency measures. For example, if the suction bucket does not achieve sufficient initial penetration, local piping may occur and jeopardise the attainment of the target penetration depth. In such a case one can consider the application of ballast to increase the downward force. If successful, this measure can lead to penetration to a depth where the suction process can begin. If not, premature refusal is the consequence. Including all individual contingencies leads to a very large event tree. Contingencies can be organised into sub-event trees per installation phase to prevent this.

6

However, many contingencies (e.g. jetting, crane actions and cyclic pumping) cannot yet be quantified as their likelihood of occurrence is low and accurate design methods are absent. Two contingencies are included in this study. Ballast material can be applied if insufficient initial self weight penetration occurs. Back-fill material (grout) can be used at refusal to fill the gap between the target and final penetration depth [15]. If a contingency can be applied successfully, it will lead to a reduction in the probability of failure of installation.

2.3. Fault tree analysis

Fault trees can be used to map conditions that need to be met for failure to occur [6]. If the probability of occurrence of each mechanism is known the probability of failure of the entire system can be analyzed. The fault tree presented in Figure 3 was developed for application in this study. Unfortunately, mutual exclusivity of failure mechanisms is hard to realise since several mechanisms can occur simultaneously, while the correlation of failure mechanisms is difficult to determine due to the non-alignment of design methods.

Installation of the suction bucket fails when penetration to target depth becomes impossible due to structural failure (buckling), pumping system failure (cavitation) or the exceedance of some geotechnical limit state (eg. piping or soil plug heave) [19]. These limitations are combined into a critical suction profile which can be regarded as the maximum allowable under pressure inside the bucket cavity at each penetration depth. A range of possible failure mechanisms have been identified in previous case studies [4], [15]. Al-

though many failure mechanisms can already be predicted, it remains hard to take phenomena caused by the filter layer or laminar layers into account accurately.
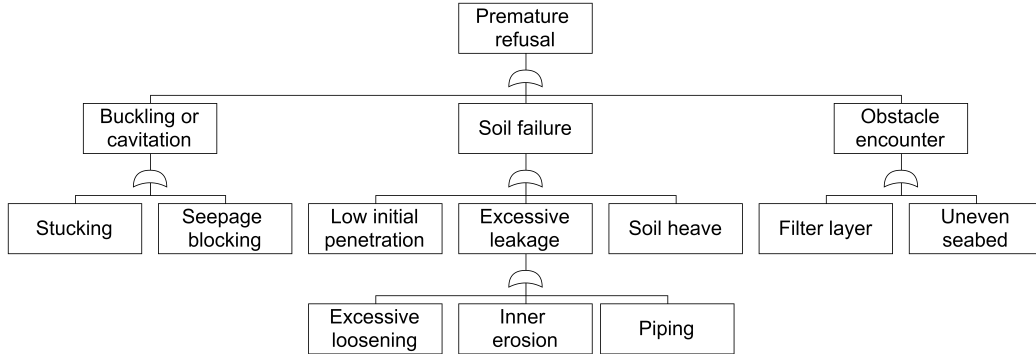

Figure 3: Fault tree for installation of suction buckets in this study

2.4. Deterministic installation design methods

Understanding how soil resistance develops during penetration forms the basis of suction bucket installation design [4]. Two main methods are available to perform such a study: the empirical CPT-based method (Cone Penetration Test) [20], [21] and the theoretical approach by Houlsby & Byrne [16]. Both methods are based on open-ended pile design and compute the soil resistance as the sum of skirt friction and the end-bearing capacity [16] (Figure 4). Both design methods consist of an assessment of two installation phases: self weight and suction-assisted penetration. The self weight penetration depth is computed by balancing the sum of end-bearing resistance (R_b) and skirt friction ($R_{i\lor o}$), with the submerged weight on the bucket (V'). In the second phase, the combined effects of the submerged bucket weight and the applied differential pressure (s) is equilibrated with the total soil re-

8

sistance accounting for any reduction caused by the applied under pressure. This vertical balance is solved for the required suction (s) at each penetration depth (h).
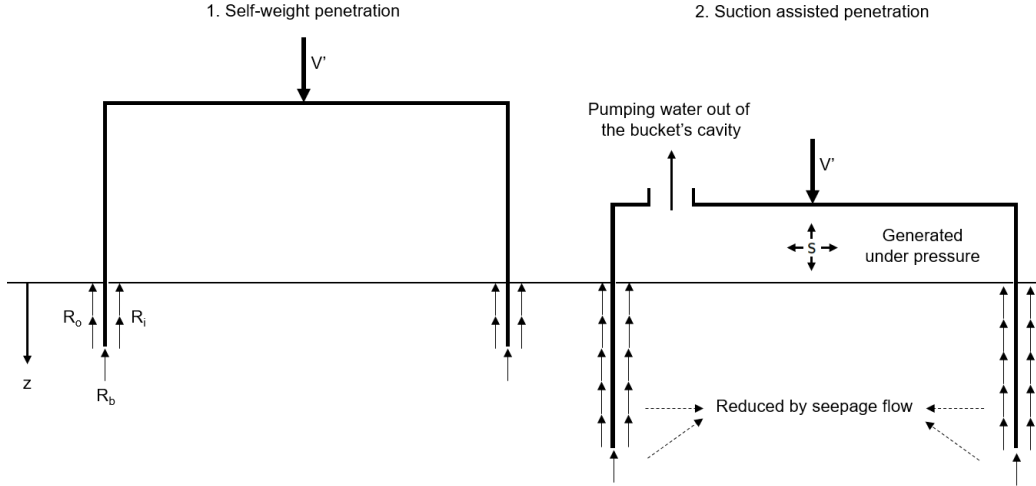
Figure 4: Installation forces during installation of buckets in cohesionless soils

2.4.1. CPT-based method

Conventional CPT-based design correlates the cone resistance obtained in a cone penetration test (q_c) to the skirt friction and end-bearing via two empirical factors. A shaft friction factor (k_f) between 0.001 and 0.003 and an end-bearing factor (k_p) between 0.3 and 0.6 is recommended in the literature [20], [21]. Specific methods correlating these empirical factors to soil properties are absent. The initial self weight penetration phase is modelled using Equation 1. The effect of under pressure (s) during phase 2 is then incorporated in the following manner. The effect of under pressure on the outer skirt is ignored. A linear reduction in value of inner skirt friction and end-bearing from initial values towards zero is assumed as under pressure

9

increases. Both resistance components become zero when the applied under pressure (s) is equal to the soil suction limit (s_c) (Equation 2) [21]. Erosion of the inner plug commences at this soil suction limit (Section 2.4.3). Empirical formulations for hydraulic failure of the soil plug (s_c) have been developed for soils of uniform permeability [19]. A thorough description of this design method is available in [21].

$$V' = \pi D_i k_f \int_0^h q_c(z)dz + \pi D_o k_f \int_0^h q_c(z)dz + (\pi D t) k_p(h) q_c(h) \qquad (1)$$

$$V' + s\left(\frac{\pi D_i^2}{4}\right) = \pi D_o k_f \int_0^h q_c(z)dz+$$

$$\left[1 - \frac{s}{s_c(h)}\right]\left[\pi D_i k_f \int_0^h q_c(z)dz + (\pi D t) k_p(h) q_c(h)\right] \qquad (2)$$

2.4.2. Houldsby & Byrne method

The Houlsby & Byrne method is based on the classical bearing capacity approach. The skirt friction is computed as a product of local horizontal effective stress (σ'_h) (calculated through the ratio of horizontal over vertical stresses, K) and the interface friction angle (δ). End-bearing is computed through end-bearing factors N_q and N_γ (Equation 3). The effective vertical stresses are enhanced by frictional forces further up the skirt and therefore develop differently on the inside (σ'_{vi}) and the outside (σ'_{vo}) of the skirt [16]. Linear development of under pressure between an applied suction (s) and a times the applied suction (as) at the skirt tip is assumed on the inside of the suction bucket. While outside, a linear under pressure dissipation from (as) at the skirt tip to zero at the seabed interface is assumed, see Equation 4.

The factor a was determined from finite element studies in soils of uniform permeability allowing for a fixed value of loosening the inner soil plug [16]. Interested readers are referred to [16] for a more thorough explanation.

$$V' = \int_o^h \left[\sigma'_{vo}(K\tan\delta)_o + \sigma'_{vi}(K\tan\delta)_i\right] dz + \left[\sigma'_v(h)N_q + \gamma'\frac{t}{2}N_\gamma\right](\pi Dt) \quad (3)$$

$$V' + s\left(\frac{\pi D_i^2}{4}\right) = \{[\sigma'_v - (1-a(h))\,s]\,N_q + \gamma'tN_\gamma\}(\pi Dt)+ \quad (4)$$

$$\int_o^h \{(\sigma'_{vo} - as)(K\tan\delta)_o + [\sigma'_{vi} - (1-a)s]\,(K\tan\delta)_i\}dz$$

2.4.3. Critical suction

After calculating the required suction, the critical suction level (the suction at which inner erosion starts to occur) is determined. Inner erosion of soil starts when the exit hydraulic gradient (i) (Figure 5) adjacent to the inner skirt exceeds some critical value imposed by gravitational forces (i_c) [19]. This is computed with the effective soil unit weight (γ') and the unit weight of water (γ_w). The exit hydraulic gradient is a function of the seepage length (l_s). Using the results of an axisymmetric finite-element seepage model and the relationship described by Equation 5 several empirical soil suction limit formulations (s_c) were developed [19]. However, work by Panagoulias et. al. (2017) suggests that these limits are too conservative [22]. Local exceedance of the critical gradient does not necessarily lead to definitive refusal since global stability might still be preserved. This matter is further discussed, for instance in [19] and [22].

$$i = \frac{s}{\gamma_w l_s} \quad , \quad i_c = \frac{\gamma'}{\gamma_w} \quad , \quad s_c = l_s\gamma' \quad (5)$$

2.4.4. Adaptations to existing design methods

All methods discussed were developed for soils that have uniform permeability with depth. Under uniform soil conditions, the change in effective stress brought about by the developed underpressure would be consistent across the site. However, when permeability varies across a site this is no longer the case and significant variation in effective stress reduction occurs. In practice there are questions over the suitability of the original methods as permeability variation and progressive soil plug loosening are to be expected [5], [23]. In this study two adaptations are made to the existing axisymmet-ric finite-element seepage models [19]. Firstly, progressive soil plug loosening is applied for the cohesionless layers where seepage occurs. The inner soil plug permeability (k_i) is multiplied with a factor (k_r) with respect to the outer permeability (k_o). Plug loosening increases with penetration depth (h) according to Equation 6 as proposed by Harireche et al. [23]. In this paper the same loosening relationship has been applied to all layers of non-cohesive material. Secondly, different layer elements are incorporated into the model thereby allowing for changes in permeability with depth.

$$k_r = \frac{k_i}{k_o} = 1.4 + 3\frac{h}{D} \qquad (6)$$

Figure 5 shows the impact of these adaptations on the developed under pressures by comparing two case studies. The left-hand side plot shows a case of constant permeability with no plug loosening. While the right-hand side plot includes a thin less permeable (80% permeability reduction) soil layer at a depth of 1 to 2 m and incorporates the effects of plug loosening ($k_r = 3.2$). The under pressures are normalized with respect to the applied under

12

pressure in the suction bucket cavity. Figure 5 shows the normalized under pressures for the two cases. Reducing the permeability causes a decrease in hydraulic head along the inner skirt wall and tip and consequently an increase in soil effective stress. Conventional design methods would under-estimate the encountered resistance in such a case. This could lead to premature refusal during installation. Plug loosening increases permeability along the wall and thereby decreases soil resistance. Both effects need to be accounted for more accurate installation design.
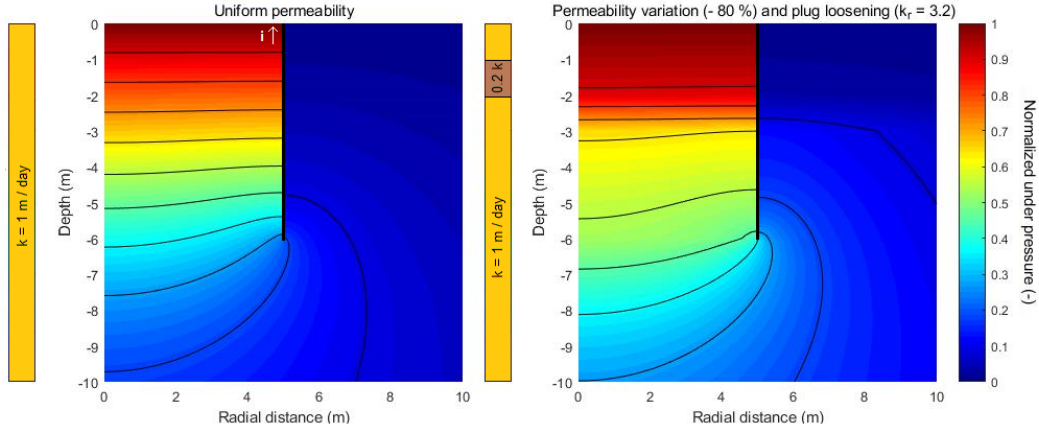
Figure 5: Impact of permeability variation and plug loosening on the seepage model output

Integrating the adapted seepage model with existing installation design methods makes them suitable for application in layered soils of varying permeability. As a consequence, model uncertainty reduces. The skirt friction and end-bearing resistance variation in both methods is carried out proportionate to the change of enhanced vertical effective stresses (σ'_{vi} and σ'_{vo}) by the applied under pressure (s) [16]. The hydraulic head difference over the bucket wall always scales linearly with the applied under pressure. This

13

means that a seepage analysis needs to be performed once per penetration depth and installation design becomes an iterative procedure, see Figure 6 and Appendix Appendix B.1.
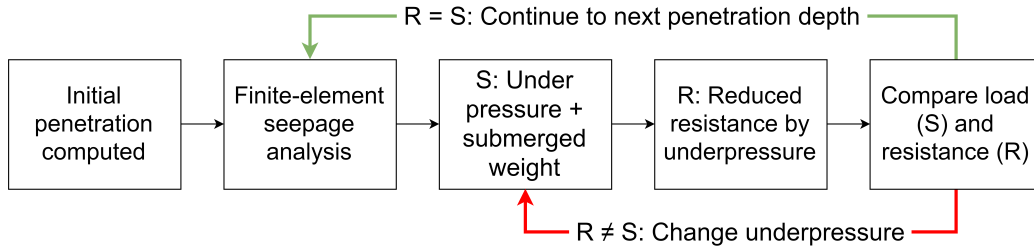

Figure 6: Iterative procedure due to integrating FEM seepage analysis into design methods

3. Quantifying parametric uncertainties

This study uses a vertical random field model to describe cone resistance (q_c) variability with depth. Fitted probability density functions are used to model the variability of all other parameters. The accuracy of both of these approaches is sensitive to both soil type and layering [24]. Therefore, several approaches are considered to ensure representative layers are identified.

3.1. Layer and soil type identification

The presence of soil layers which have different properties (strength, stiffness, permeability etc.) and exhibit different behavior under stress can have a large impact on the installation of suction buckets. Accurate layer identification is therefore a necessity. This study employs four distinct identification methods simultaneously: borehole logs, the soil behaviour type index, the statistical moving window method and Bartlett profiling.

Borehole logs contain the subjective interpretation made during visual examination of the samples on site (e.g. sub angular coarse grained sand). Often these logs contain additional information on the geological history of the deposit [25]. Borehole logs are valuable for identifying small layers or lenses which might not be captured by a cone penetration test. The soil behaviour type index (I_c) is computed after normalising the cone tip resistance (q_c) and the shaft friction (f_s) with effective stress (Q_t, F_r) (Equation 7 and 8). It can be used to give a first indication of the soil type based on an interpretation of the Robertson classification chart [26].

$$I_c = \left[(3.47 - \log Q_t)^2 + (\log F_r + 1.22)^2 \right]^{0.5} \tag{7}$$

$$Q_t = \frac{q_t - \sigma_{v0}}{\sigma'_{v0}} \quad , \quad F_r = \left[\frac{f_s}{q_t - \sigma_{v0}} \right] 100\% \tag{8}$$

Both the statistical moving window method [27] and Bartlett profiling [28] utilise a moving window to examine the average soil variance over the cone resistance profile. The moving window method computes the coefficient of variation (COV) of the cone resistance in each window. The objective of this method is to identify homogeneous soil units from such a profile. Bartlett profiling computes a statistical value (B_{stat}) per depth based on comparing the standard deviation of both halves of the sampling window (σ_{b1}, σ_{b2}), see Equations 9 and 10. Peaks within the profile indicate a change in soil behavior. The width of the peaks and troughs in both moving window methods, depend on the standard deviation of the cone resistance, the number of measurements (m_b) and the chosen window width.

$$B_{stat} = \frac{2.30259(m_b - 1)}{C_b} \left[2 \log \left(\frac{\sigma_{b1}^2 + \sigma_{b2}^2}{2} \right) - \left(\log(\sigma_{b1}^2) + \log(\sigma_{b2}^2) \right) \right] \quad (9)$$

$$C_b = 1 + \frac{1}{2(m_b - 1)} \quad (10)$$

None of the four methods mentioned fully correspond to one another. The accuracy of the borehole log depends on the loggers experience. Neither of the moving window methods has an objective threshold to distinguish layer boundaries. As a consequence distinct peaks and troughs in the profile must be used. Furthermore, both moving window methods are sensitive to the choice of window width. Figure 7 shows that enlarging the window results in a significant decrease of distinct peaks, while decreasing the window width will result in more peaks indicating layer boundaries, some of which may not exist. Both moving window methods are challenging to apply at shallow depths, since the magnitude and variation of the cone resistance are typically low. While the soil behavior type index (I_c) does have objective identification thresholds, it can fail to capture a change in the gradient of the cone resistance trendline. This can result in an overestimation of the of cone resistance variation when constructing a random field model (Section 3.2).
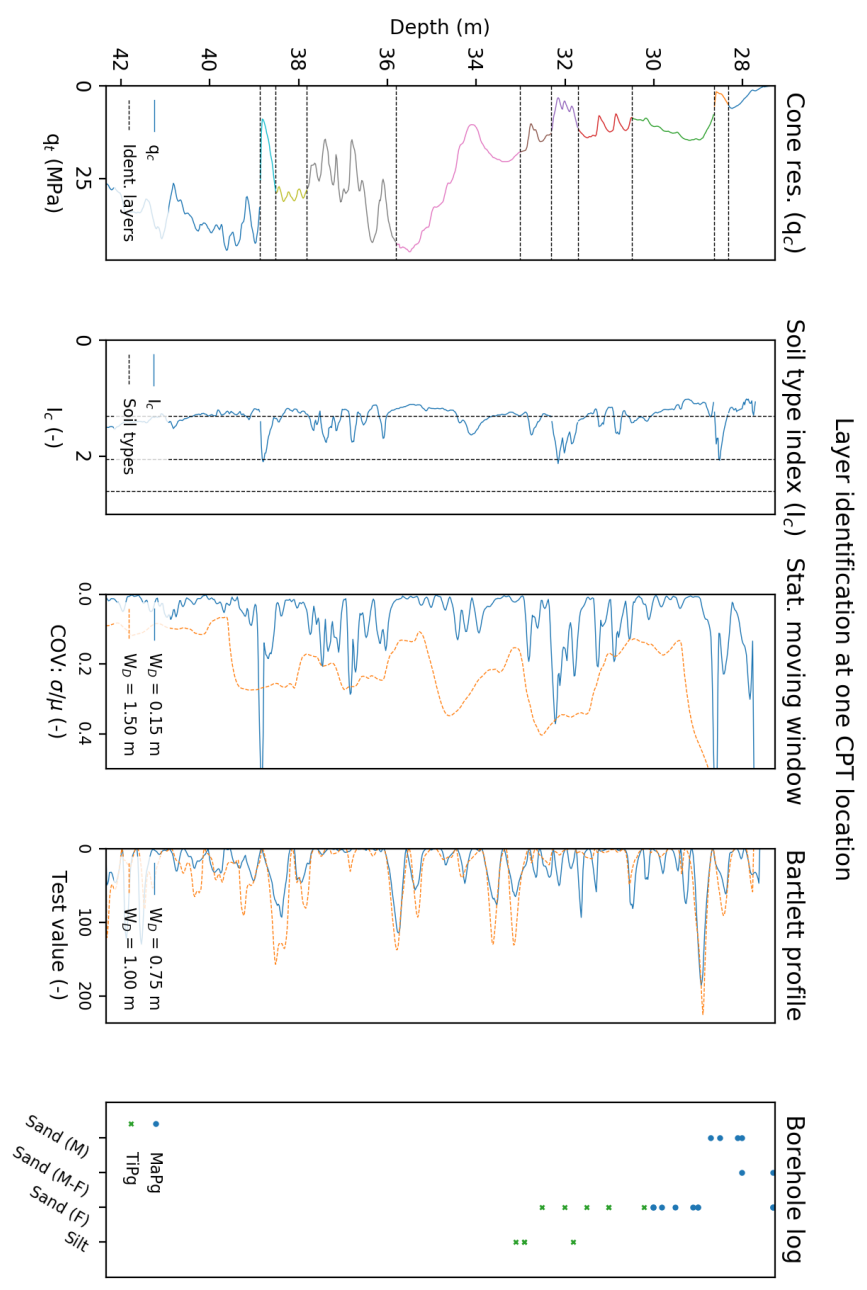
Figure 7: Comparison of layer identification by the four methods applied in this study

None of the four identification methods are without flaws. To verify the layer identification process the CPT data from each layer with correspond-ing second moments (standard deviations) can be depicted on a Robertson classification chart. This allows for further optimisation of layer boundaries by selecting boundary locations which minimise second moments. It can also be used to merge two identified layers which turn out to have very similar characteristics. This avoids overcomplicating the analysis of installation per-formance. Figure 8 shows the second moment plot for the layers identified in Figure 7. At this location eleven layers of different behaviour were identified by means of all four methods described. Figure 8 shows a distinct difference in both the mean and its variation for all neighbouring layers.
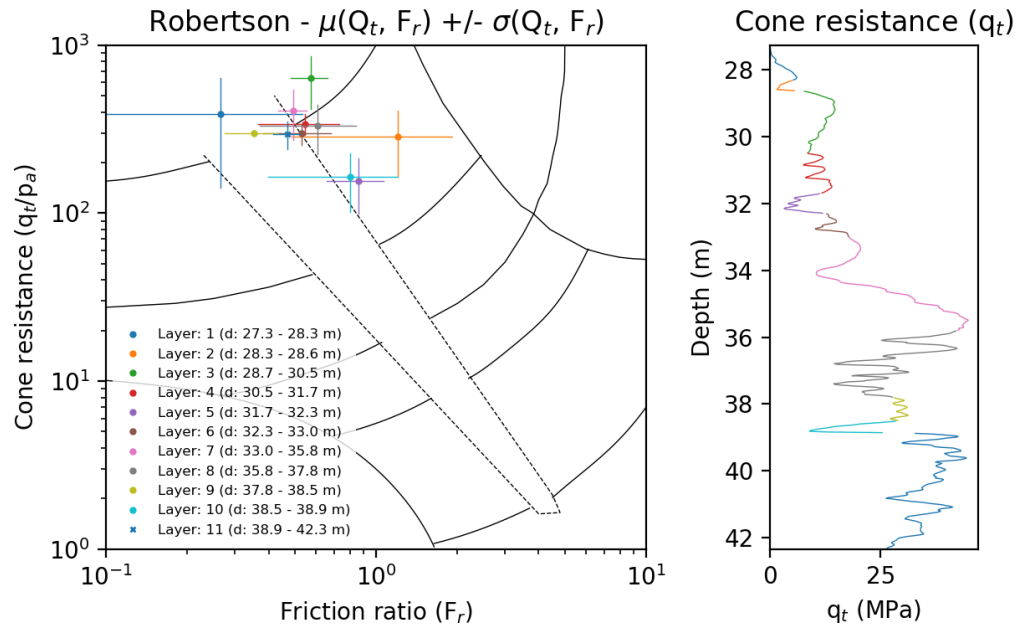

Figure 8: Second moment classification chart for validation of layer identification [26]

3.2. Random field modelling of cone resistance

A random field model can be constructed for any stochastic process which can be described by a trend and a variation with zero mean about that trend [29]. The vertical variability of the cone resistance within each layer is described by its own random field, see Figure 9. Two prerequisites should be satisfied in order to ensure applicability [24]:

1. Soil layers used should be physically homogeneous in their behavior;
2. The variations of soil properties about their respective trendlines should be weakly stationary.

Proper layer identification as elaborated on in Subsection 3.1 can assure meeting the prerequisite on physical homogeneity. Weakly stationary variation along the trendline indicates that there is no trendline incorporated in the variation profile which therefore means variation is independent of its location within the layer. Besides checking that the variability oscillates about a zero mean when detrended, no generally applicable objective methods are currently available for the assessment of weak stationarity [28].

Each layer in a random field model requires a trendline describing the mean (μ) and a standard deviation (σ), a scale of fluctuation (δ_v) combined with a corresponding theoretical autocorrelation function, R(τ) describing the variation [28]. The latter describes the spatial correlation of variation within the profile [29]. To obtain this for a given layer at a location the following procedure is applied [30]. First, empirical autocorrelation func-tions are determined for all variability profiles obtained from different CPT's

19
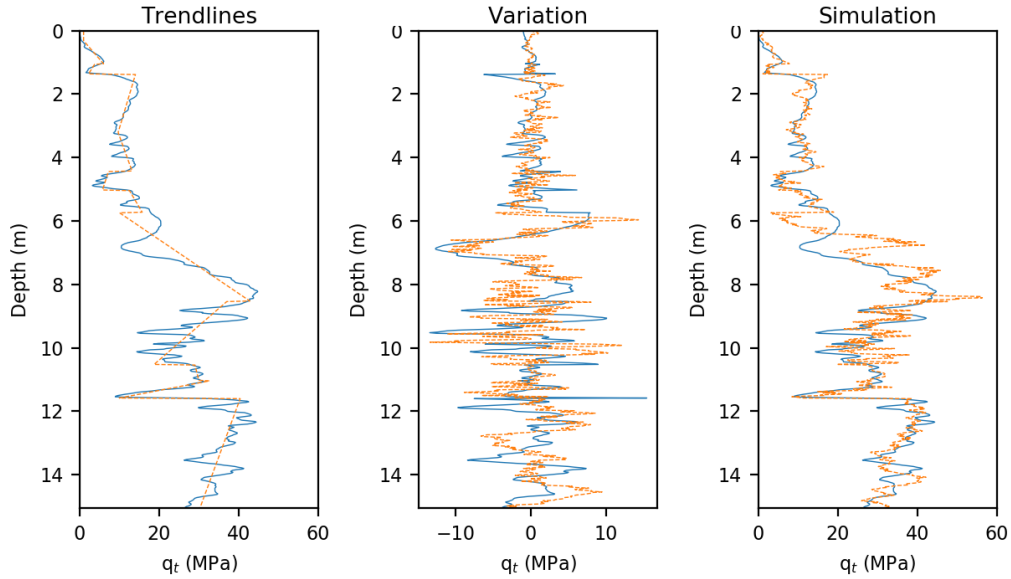
Figure 9: Example of vertical CPT random field modelling in this study

within the same soil layer according to Equation 11. The mean empirical autocorrelation is then calculated and theoretical autocorrelation models are fitted to it using a least squares approach (Table 3.2). The best fitting theoretical model is selected with its corresponding scale of fluctuation (δ_V) and is used for all further simulations, see Figure 10 and Appendix B.2.

Three criteria are considered to match soil layers from different CPTs in order to ensure that the correct data is used for determining the mean empirical auto-correlation:

1. The layers should have a similar soil behavior type index ($\Delta I_c < 5\%$);
2. The layers should belong to the same geological deposit;
3. The layers should overlap in depth.

Applying these criteria allows for the generation of theoretical auto-correlation functions which are based on the empirically fitted curves representative of the site at large, see Figure 10.

$$\rho(\tau_j) = \frac{1}{\sigma^2(n-j)} \sum_{i=1}^{n-j} (X_i - \mu)(X_{i+j} - \mu) \tag{11}$$

Model	Equation	Scale of fluct.
Single exponential	$R(\tau) = \exp(-\lambda \, |\tau|)$	$\delta_v = 2 \, / \, \lambda$
Binary noise	$R(\tau) = 1 - c|\tau|$ (if $|\tau| = 1/c$)	$\delta_v = 1 \, / \, c$
Cosine exponential	$R(|\tau|) = \exp(-b|\tau|) \cos(b\tau)$	$\delta_v = 1 \, / \, b$
Second-order Markov	$R(|\tau|) = (1 + d|\tau|) \exp(-d|\tau|)$	$\delta_v = 4 \, / \, d$
Squared exponential	$R(|\tau|) = \exp[-(\alpha \, \tau)^2]$	$\delta_v = \sqrt{\pi} \, / \, a$

Table 1: Theoretical autocorrelation models common in geotechnical data analysis [28]
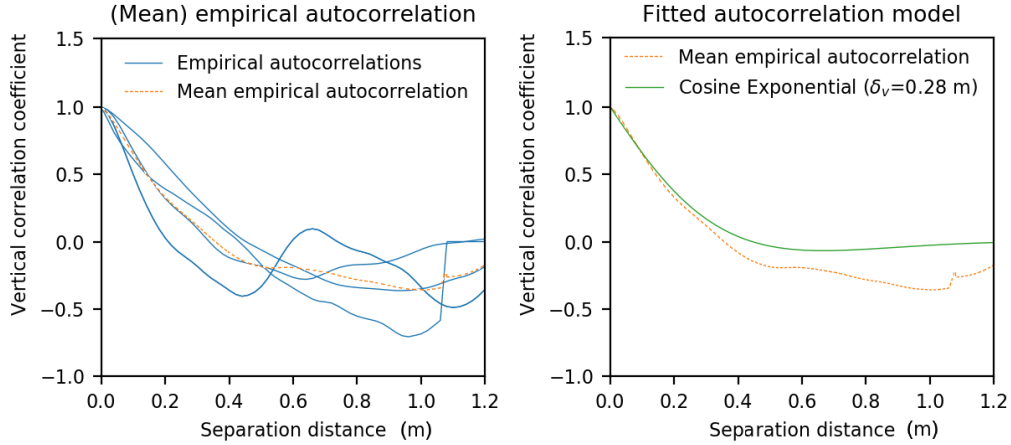

Figure 10: Fitting auto-correlation model to differently sized but matching soil units

21

Many current vertical random field studies consider few soil layers and model large outliers as cone resistance variation [31], [32]. This is feasible for very homogeneous soils over depth and closely spaced cone penetration tests. Offshore cone penetration tests are typically positioned further apart. Additionally, the presence of thin laminar layers can severely impact layer permeabilities and can have serious consequence on the installation design of suction buckets and therefore should not be ignored. These arguments emphasize the need for one random field per soil layer with corresponding trendlines and variance description (as in Figure 9).

Negative cone resistances are a physical impossibility and therefore must not be simulated [10]. To prevent this, simulated Gaussian processes are transformed into the log-normal domain. Caution should be exercised at locations where the fitted linear trendline values are close to zero or negative. This can happen if the trendline for the uppermost layer is not constrained to the positive domain. In such cases it will be difficult to avoid simulating negative cone resistances. The trendline should always be corrected to only contain small near-zero positive values to avoid this.

3.3. Continuous probability density functions (PDF)

Parameter estimates are obtained from the results of laboratory or field tests via direct measurement or correlation (Table 3.3). The required parameters are treated as random variables as they can have different values under different conditions which have a different probability of occurrence [33]. The probability of occurrence is described by a continuous PDF. Different soil types form under different conditions and can have a difference in

geotechnical properties as a consequence. Therefore parameter estimates are grouped per soil type. Histograms are plotted for different parameter groupings and soil types to ensure that the resulting continuous distributions are uni-modal. Discrete variability is then quantified using both histograms and fitted empirical Cumulative Density Functions (CDFs). Figure 11 shows the calculated permeability CDF for the different soil types. The result is as expected since finer soils have a lower permeability. As previously discussed, Gaussian distributions are not suitable for modelling parameters which cannot have values in the negative domain. Several PDFs are fitted and assessed for each parameter.

Variable	Symbol	Type	Used
Soil unit weight	γ'	Measurements	-
Relative density	R_D	Correlation	Jamiolkowski [34]
Angle of internal friction	ϕ	Correlation	Andersen [35]
Permeability	k	Correlation	Kozeny-Carman [36]
Interface friction angle	δ	Estimate	$\delta = \phi - 5^o$ [37]
Stress ratio	K	Estimate	K = 1-2 [38]

Table 2: Parameter estimation methods applied on the case study dataset

All probable distributions are fitted using the maximum likelihood estimator to determine shape and location factors. Two 'goodness of fit tests' are applied to objectively assess the accuracy of the fit. The Pearson χ^2 test compares the shape of the continuous PDF to its normalised histogram. The weighted error is checked against a predetermined threshold based on the number of estimates and the χ^2 distribution [39]. The Kolmogorov-Smirnov
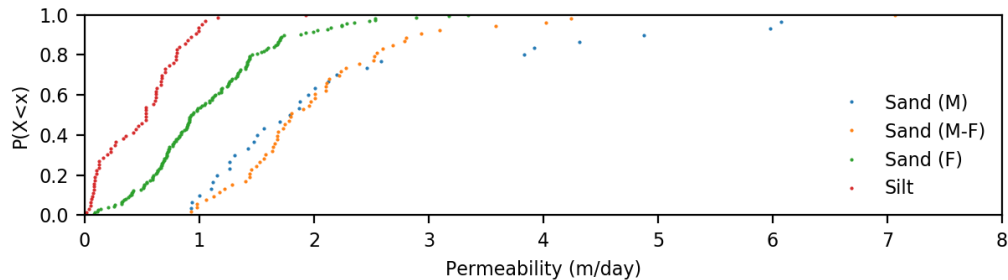
Figure 11: Different empirical cumulative density functions of estimated permeability

Function	Variables	Domain	Remark
Gaussian distribution	ϕ, γ'	All	Common
Log-normal distribution	k, ϕ, γ'	Positive	Common
Weibull	k, ϕ	Positive	Common
Beta	k, ϕ	Positive	Flexible shape
Exponential	k	Positive	Decaying, starts at 0
Uniform distribution	K	All	Discontinuous

Table 3: Probable continuous probability density functions selected for fitting procedure

test determines the maximum error between the empirical and continuous CDF. It compares this to a threshold which depends on the number of parameter estimates [40]. The score of both tests is normalised by their respective threshold and averaged afterwards. The fitted continuous distribution which scores best on average is used to describe the variability of a parameter in a given soil type. A minimum of 30 samples is set as the lowest threshold for Pearson's χ^2 'goodness of fit' test. Otherwise the mean value is used as a deterministic estimate. Figure 12 shows the procedure for modelling the variability of the permeability of medium to fine sands based on 51 estimates. The log-normal distribution showed the best fit.
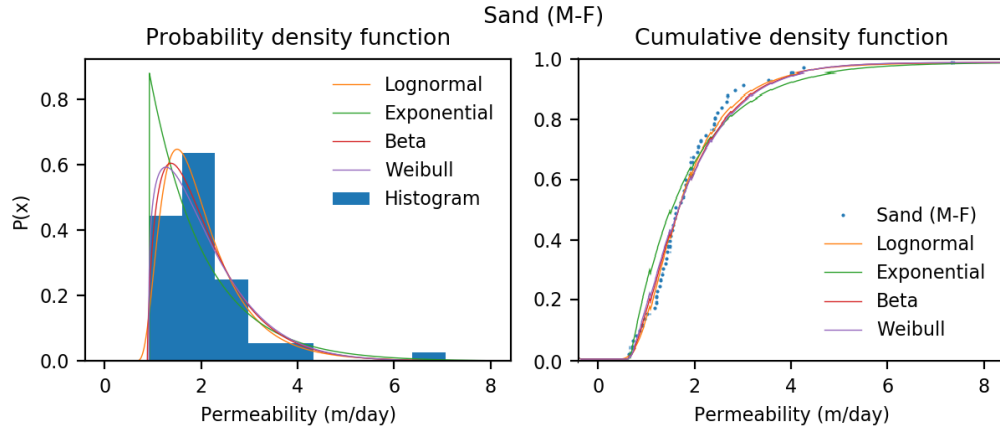
24

Figure 12: Fitted continuous distributions for permeability of medium to fine sands

4. Quantitative reliability analysis

In this section, the quantified parametric uncertainties from Section 3 will be implemented into the developed design methods for different failure mechanisms and contingencies (Section 2). The results provide insight into the impact of uncertainties on installation design.

4.1. Monte Carlo simulation

Almost every design problem can be simplified into a combination of a load (S) and a resistance (R). Feasibility can likewise be expressed by the limit state (G = R - S). A limit state (G < 0) value below zero corresponds to a failure scenario, while (G > 0) represents a safe design. [6]. In this study, the resistance is represented by the critical suction profile (s_c) and the load by the required suction profile (s_r). Both the empirical CPT-based method and the theoretical approach of the Houlsby & Byrne method are used to determine required suction profiles. Each quantifiable failure mechanism (e.g.

buckling, cavitation or inner erosion) is expressed as the maximum allowable underpressure at that depth. This forms a limit state over depth which may not be exceeded by the applied underpressure.

The original limit state formulation is not usable for continuous processes like suction bucket installation, as failure could occur at any depth. Therefore the smallest absolute difference does not necessarily represent the point most likely to fail. The relative magnitude dictates the reliability instead. The limit state is normalised by the critical suction profile to find the point which is relatively closest to failure (Equation 12).

$$G = s_c - s_r \quad \rightarrow \quad G = 1 - \frac{s_r}{s_c} \tag{12}$$

The probability of failure can be assessed in a quantitative reliability analysis. Suction bucket installation is a multi-dimensional problem due to its many input parameters. This hinders application of direct integration or first order reliability methods [41]. Regular Monte-Carlo simulation is the most suitable method for these types of problems; as it allows for the direct input of advanced probabilistic distribution types and is accurate when sampled extensively. Parameters are randomly sampled from their representative distributions to construct design profiles. The number of iterations which fail divided by the total amount of iterations carried out represents the probability of failure (Figure 13 and Appendix B.3).
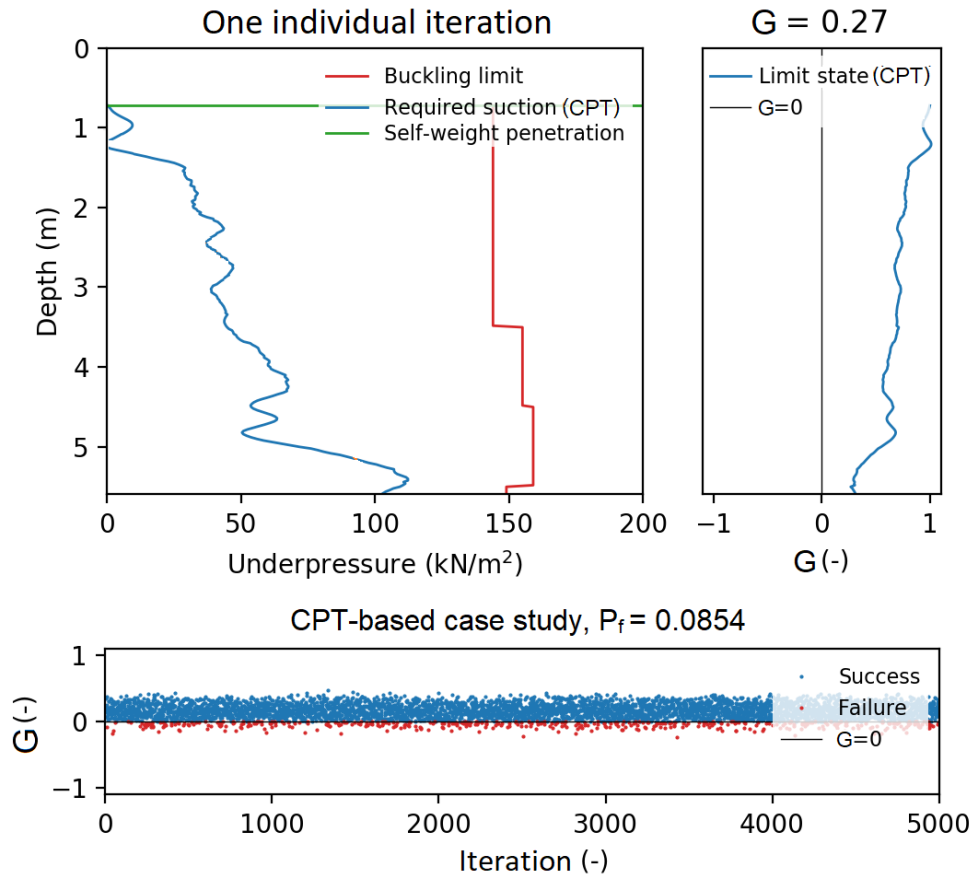
Figure 13: Monte Carlo simulation for probability of buckling failure at one location

One drawback of Monte-Carlo simulation is that the time taken to assess low probability events can become significant, particularly when a high degree of accuracy is required. Optimised methods for faster computation (e.g. Markov Chain Monte Carlo, Importance Sampling etc.) do exist and are applied in literature [42]. However, when used in combination with random field models and a depth dependent limit state (e.g. composed critical suction profiles) any time savings are lost.

4.2. Feasibility assessment

The probabilities of failure due to buckling, exceeding soil suction limits and cavitation are assessed using Monte-Carlo simulations of 5,000 iterations. An example for a bucket with a diameter (D) of 10 m, final penetration depth (h) of 5.5 and wall thickness (t) of 45 mm is presented in Figure 13. In this case the CPT-based method (adapted for layers of varying permeability) is applied. The effect of contingency measures such as the application of ballast and backfill material are included where appropriate to reduce probabilities of failure accordingly (Section 2.2). The observed failure probabilities are high. The large model uncertainty contributes to this as: 1). The soil suction limits are believed to be too conservative and the impact of many contingency measures cannot be quantified [22]. 2). The error in CPT results can be quite high, as CPT cones sample a relatively small area compared to that of the suction bucket. Therefore, they register the significance of occluded pebbles etc. as more important than they actually are when scaled up. 3). The model error in measuring permeability and soil friction angles is significant, particularly given the scale of magnitude of the change these parameters undergo during loading. Aside from model error, the lack of sufficient sur-vey data to accurately model horizontal variability adds uncertainty to the analysis. Lateral variability of soil strength and permeability cannot be included, which eliminates the opportunity of including some aspects relevant to suction bucket installation (e.g. preferential flow and horizontal strength variation) [15].

28

The importance of a quantitative reliability analysis becomes clear when one compares the results to that of conventional design methods. In current driveability practice, it is common to construct lower and upper bounds using a standard safety factor (γ=1.25) [43]. Taking 95% reliability intervals, as recommended by Eurocode 7 for underpressure at each depth, the output of the Monte-Carlo simulation could be used instead of a conventional design approach. In the left plot of Figure 14 a deterministic estimate and the outcome of all iterations in the Monte Carlo simulation are presented. These are then translated to a lower and upper bound using the conventional method (γ = 1.25) and 95% reliability intervals in the right plot (Appendix B.3). As the bandwidth of the conventional method is consistently lower than that of the reliability based approach, it would appear that the selected safety factor is non-conservative with respect to the quantified uncertainties and carries a greater failure probability.
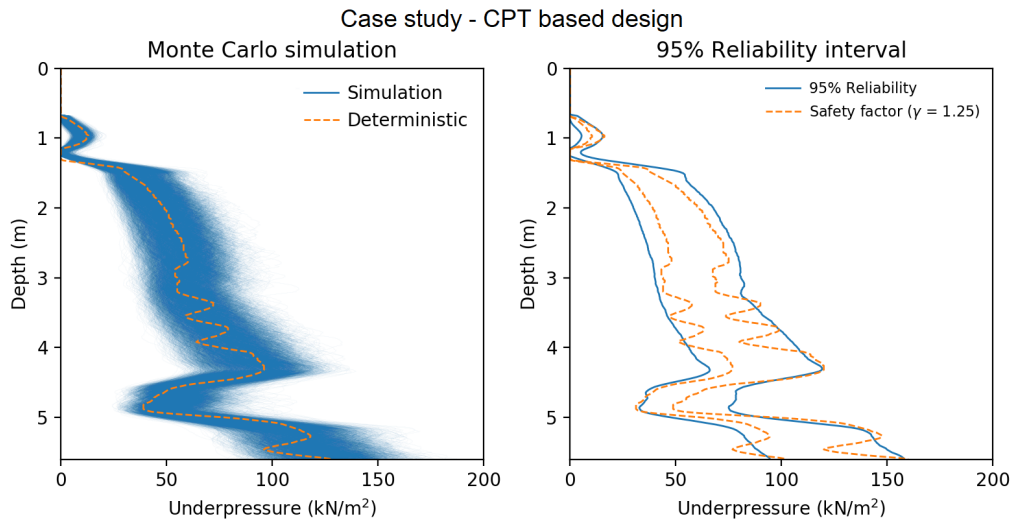

Figure 14: Comparison of deterministic design with a safety factor to a reliability interval

4.3. Sensitivity analyses

Failure mechanisms develop when an unfavorable load resistance envelope occurs at a location. The sampled parameters and limit state profiles of a Monte-Carlo simulation can be used to assess the origin of generated failure situations. Failure is observed when simulated soil resistances are high. When a high soil resistance is observed the angle of internal friction (ϕ) and the ratio of horizontal stress (K) are high too. The probability of failure is therefore very sensitive to any change in these parameters.

The influence of parameter estimates as well as the incorporation of variability can be determined with a quantitative reliability analysis. Figure 15 illustrates this using the Houlsby & Byrne design method. In the left plot the median profiles of all samples with particular stress ratios (high and low) are plotted. These are extracted from the bulk of iteration results during a Monte Carlo analysis. One can see that the stress ratio (K) estimate has a large impact on the outcome profile. This is unfortunate given the great difficulty in accurately estimating this parameter in cohesionless soils [17]. However, it also shows the power of reliability analyses in influencing decision makers to perform more field tests.

The right graph of Figure 15 gives an example of the impact of parametric variability on the results. Two 95% confidence intervals are plotted showing the results of two Monte-Carlo analyses. The first Monte-Carlo analysis was executed with varying permeability estimates sampled from the previously determined distributions. The second analysis was executed using the ex-
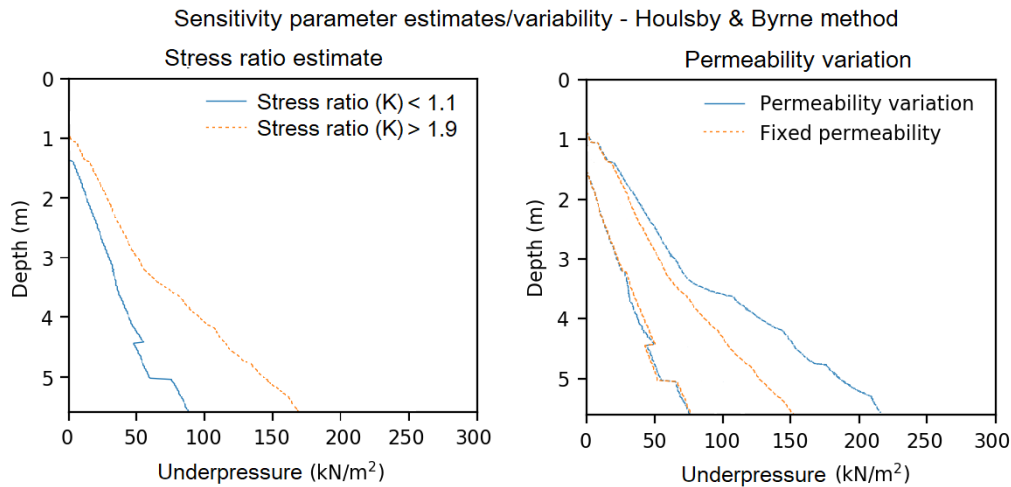
Figure 15: Influence of stress ratio estimate and permeability variation on design outcomes

pected values from the same distributions. One can see that incorporating the variation of permeability has significant impact on the upper bound of the confidence interval, naturally having this much uncertainty in your underpressure development will led to a less reliable installation. Combined with the fact that it can be used to assess and simulate governing failure mechanisms one can state that incorporating permeability variation is required.

Figure 16 shows simulated failures and corresponding histograms of sampled permeabilities. The low sampled permeability in layer three indicates that the governing failure mechanism is seepage blocking. This low permeability layer prevents the generation of underpressures beneath it and therefore fails to reduce soil resistance which can cause premature refusal. Slight deviations towards higher permeability in lower layers are present too and

indicate the occurrence of stucking. In such cases high permeability layers hinder the generation of sufficient underpressure. As a consequence the soil resistance is insufficiently reduced to allow for further penetration [15]. Understanding governing failure mechanisms can help in planning contingencies as well as setting the scope for future site investigations.
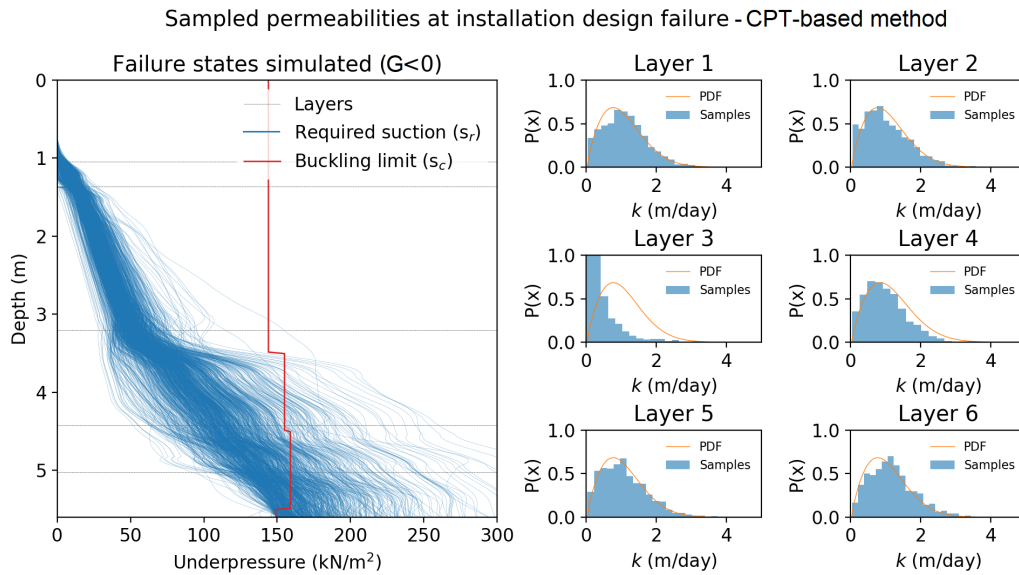

Figure 16: Parametric study leading to identification of governing failure mechanisms

5. Conclusion and discussion

This study objectively quantified variability of geotechnical parameters and incorporated it into two existing design methods for suction bucket installation. The impact of considering permeability variations within layers and between layers was shown to be highly significant and should be considered in practice. The existing installation design methods were adapted to integrate a finite-element seepage model and progressive plug loosening, thus making them suitable for application in layered soils of varying per-meability. As a consequence, model uncertainty reduced. Application of reliability-based design led to an improved understanding of the expected failure mechanisms through investigating model sensitivities. Additionally, it provides a basis for accurately determining conservatism, thereby reducing the chance of unexpected failure.

Suction bucket installation design research typically uses ideal data-sets with homogeneous soil conditions. This study showcases the steps necessary to adapt these methods for non-homogeneous sites such as those commonly found in practice. In such conditions, layer and soil type identification are essential in order to avoid over- or underestimation of the soil resistance during installation. Integrating these features into installation design accounts for several unfavourable effects (e.g. seepage blocking and stucking), which would otherwise not be considered. This helps to more accurately predict the occurrence of premature refusal and increases the safety margin in installation design. Four layer identification methods were presented and contrasted in this research. It was found they were seldom in complete agree-

ment, but were best utilised in combination with each other. It was shown that a statistical sound application of vertical random field modelling of the cone resistance requires a more extensive check on its prerequisites (homogeneity and stationarity). Due to the shallow embedment depth of suction buckets, assuming homogeneity or stationarity without checking can lead to substantial over- or under estimation of the cone resistance and hence the resistance calculated in suction bucket design. Each layer needs to be properly identified and assigned its own random field. This is challenging in practice since the accuracy of a vertical random field is hard to assess without many closely spaced CPTs. Probability density functions provide an excellent tool for modelling the variability of soil parameter estimates. Using 'goodness of fit' tests such as the Pearson χ^2 and the Kolmogorov-Smirnov test is recommended since they objectively assess distribution fit and suitability.

Integrating Monte Carlo simulation outputs into the developed fault tree resulted in high estimates of the probability of installation failure. The high failure probability can partly be attributed to conservatism in the computation of the limit state (critical suction). Currently, soil limits are set at under-pressure values which are computed based on the onset of erosion. However, the onset of erosion is not necessarily synonymous with installation failure. Future model tests should give more insight into the geometric extent of critical gradients at failure.

The reliability study as well as the installation design method can be improved by assessing other design aspects as well. For example at this point, it is not possible to calculate the influence of a filter layer on the pen-etration process. Furthermore, the CPT-based method can be improved by developing an estimation method for the empirical coefficients based on back-calculation using measured field data of similarly shaped foundations. This study shows that 95 % reliability intervals can be used to verify adaptations made to installation design or parameter estimates. If the bandwidth of an improved method consistently decreases towards the measured output during installation one can verify whether the adaptations made can be considered an improvement. Mutual exclusivity of failure mechanisms is hard to realise since several failure mechanisms can occur simultaneously while at present their correlation is difficult to determine due to the non-alignment of design methods. Better design method alignment would allow this to be accounted for within a risk based framework.

In practice, variability of soil properties is difficult to determine without extensive site investigation. Without knowing the horizontal variability of soil properties it is impossible to quantify preferential flow or spatially average soil strength across the diameter of a bucket. Both are likely to significantly change design outcomes and their probability of failures. In practice multiple buckets are often installed as the foundation for a jacket structure, which supports the wind turbine. There is a need to investigate interaction effects and develop more accurate modelling of horizontal variability, in order to assess the feasibility of such structures holistically as a system.

6. References

[1] T.-I. Tjelta, The suction foundation technology, in: V. Meyer (Ed.), Proceedings of the 3rd International Symposium on Frontiers in Offshore Geotechnics, CRC Press, Oslo, 2015, pp. 85–93.

[2] L. Arany, S. Bhattacharya, Simplified load estimation and sizing of suction anchors for spar buoy type floating offshore wind turbines, Ocean Engineering 159 (2018) 348–357.

[3] Wind Europe, The European offshore wind industry - Key trends and statistics 2017, Technical Report, Wind Europe, Brussels, Belgium, 2017.

[4] A. Foglia, L. B. Ibsen, Bucket foundations: a literature review, Department of Civil Engineering, Aalborg University, Denmark, 2014.

[5] M. N. Tran, M. F. Randolph, D. W. Airey, Installation of Suction Caissons in Sand with Silt Layers, Journal of Geotechnical and Geoenvironmental Engineering 133 (2007) 1183–1191.

[6] J. T. Christian, Geotechnical Engineering Reliability: How Well Do We Know What We Are Doing?, Journal of Geotechnical and Geoenvironmental Engineering 130 (2004) 985–1003.

[7] S. Lacasse, F. Nadim, Probabilistic geotechnical analyses for offshore facilities, Georisk: Assessment and Management of Risk for Engineered Systems and Geohazards 1 (2007) 21–42.

[8] J. T. Christian, C. C. Ladd, G. B. Baecher, Reliability Applied to Slope Stability Analysis, Journal of Geotechnical Engineering 120 (1994) 2180–2207.

[9] K.-K. Phoon, F. H. Kulhawy, Evaluation of geotechnical property variability, Canadian Geotechnical Journal 36 (1999) 625–639.

[10] G. A. Fenton, D. V. Griffiths, Bearing-capacity prediction of spatially random c - ϕ soils, Canadian Geotechnical Journal 40 (2003) 54–65.

[11] A. I. H. Malkawi, W. F. Hassan, F. A. Abdulla, Uncertainty and reliability analysis applied to slope stability, Structural Safety 22 (2000) 161–187.

[12] K.-K. Phoon, F. H. Kulhawy, Characterisation of model uncertainties for laterally loaded rigid drilled shafts, Géotechnique 55 (2005) 45–54.

[13] C. Reale, J. Xue, K. G. Gavin, System reliability of slopes using multimodal optimisation, Géotechnique 66 (2016) 413–423.

[14] T. H. Wu, W. H. Tang, D. A. Sangrey, G. B. Baecher, Reliability of Offshore Foundations - State of the Art, Journal of Geotechnical Engineering 115 (1989) 157–178.

[15] H. Sturm, Design Aspects of Suction Caissons for Offshore Wind Turbine Foundations, in: S. Yunsup (Ed.), International Conference on Soil Mechanics and Geotechnical Engineering, volume 19, ISSMGE Technical Committee TC 209, Seoul, South Korea, 2017, pp. 45–63.

[16] G. T. Houlsby, B. W. Byrne, Design procedures for installation of suction caissons in sand, Proceedings of the Institution of Civil Engineers - Geotechnical Engineering 158 (2005) 135–144.

[17] B. van Dijk, Design of suction foundations, Journal of Zhejiang University 19 (2018) 579–599.

[18] R. V. Whitman, Evaluating Calculated Risk in Geotechnical Engineering, Journal of Geotechnical Engineering 110 (1984) 143–188.

[19] L. B. Ibsen, C. L. Thilsted, Numerical Study of Piping Limits for Suction Installation of Offshore Skirted Foundations an Anchors in Layered Sand, in: S. Gourvenec, D. White (Eds.), Frontiers in Offshore Geotechnics II, CRC Press/Balkema, 2010, pp. 421–426.

[20] K. H. Andersen, H. P. Jostad, R. Dyvik, Penetration Resistance of Offshore Skirted Foundations and Anchors in Dense Sand, Journal of Geotechnical and Geoenvironmental Engineering 134 (2008) 106–116.

[21] M. Senders, M. F. Randolph, CPT-Based Method for the Installation of Suction Caissons in Sand, Journal of Geotechnical and Geoenvironmental Engineering 135 (2009) 14–25.

[22] S. Panagoulias, B. F. J. van Dijk, T. Drummen, A. Askarinejad, F. Pisano, Critical Suction Pressure During Installation of Suction Caissons in Sand, in: Offshore Site Investigation and Geotechnics: 'Smarter Solutions for Future Offshore Developments', volume 8, Society of Underwater Technology, Londen, 2017, pp. 570–577.

[23] O. Harireche, M. Mehravar, A. M. Alani, Soil conditions and bounds to suction during the installation of caisson foundations in sand, Ocean Engineering 88 (2014) 164–173.

[24] M. Uzielli, S. Lacasse, F. Nadim, K.-K. Phoon, Soil variability analysis for geotechnical practice, in: International Workshop on Characterisation and Engineering Properties of Natural Soils, volume 3, Taylor and Francis, 2006, pp. 1653–1752.

[25] J. Peuchen, Site characterization in nearshore and offshore geotechnical projects, in: R. Q. Coutinho, P. W. Mayne (Eds.), Geotechnical and Geophysical Site Characterization 4, volume 1, CRC Press, 1 edition, 2013, pp. 83–111.

[26] P. K. Robertson, Cone penetration test (CPT)-based soil behaviour type (SBT) classification system an update, Canadian Geotechnical Journal 53 (2016) 1910–1927.

[27] M. Uzielli, G. Vannucchi, K.-K. Phoon, Random field characterisation of stress-nomalised cone penetration testing parameters, Géotechnique 55 (2005) 3–20.

[28] K.-K. Phoon, S.-T. Quek, P. An, Identification of Statistically Homogeneous Soil Layers Using Modified Bartlett Statistics, Journal of Geotechnical and Geoenvironmental Engineering 129 (2003) 649–659.

[29] R. Rackwitz, Reviewing probabilistic soils modelling, Computers and Geotechnics 26 (2000) 199–223.

[30] M. Lloret-Cabot, G. A. Fenton, M. A. Hicks, On the estimation of scale of fluctuation in geostatistics, Georisk: Assessment and Management of Risk for Engineered Systems and Geohazards 8 (2014) 129–140.

[31] P. Doherty, K. G. Gavin, Statistical review of CPT data and implications for pile design, in: P. K. Robertson, P. W. Mayne (Eds.), Proceedings of the 2nd international Symposium on Cone Penetration Testing, volume 3, CPT 10, Huntington Beach, California, 2010.

[32] L. J. Prendergast, C. Reale, K. G. Gavin, Probabilistic examination of the

change in eigenfrequencies of an offshore wind turbine under progressive scour incorporating soil spatial variability, Marine Structures 57 (2018) 87–104.

[33] F. M. Dekking, C. Kraaikamp, H. P. Lopuhaä, L. E. Meester, A Modern Introduction to Probability and Statistics: Understanding Why and How, Springer-Verlag, London, 5th edition, 2005.

[34] M. Jamiolkowski, D. C. F. Lo Presti, M. Manassero, Evaluation of relative density and shear strength of sands from CPT and DMT, Soil Behaviour and Soft Ground Construction (2003) 201–238.

[35] K. H. Andersen, K. Schjetne, Database of Friction Angles of Sand and Consolidation Characteristics of Sand, Silt, and Clay, Journal of Geotechnical and Geoenvironmental Engineering 139 (2013) 1140–1155.

[36] W. D. Carrier III, Goodbye, Hazen; Hello, Kozeny-Carman, Journal of Geotechnical and Geoenvironmental Engineering 129 (2003) 1054–1056.

[37] B. M. Lehane, R. J. Jardine, A. J. Bond, R. Frank, Mechanisms of Shaft Friction in Sand from Instrumented Pile Tests, Journal of Geotechnical Engineering 119 (1993) 19–35.

[38] K. G. Gavin, Use of CPT for the design of shallow and deep foundations on sand, in: M. Hicks, F. Pisano, J. Peuchen (Eds.), Cone Penetration Testing 2018: Proceedings of the 4th International Symposium on Cone Penetration Testing, CRC Press, Delft, 2018, pp. 45–61.

[39] R. L. Plackett, Karl Pearson and the Chi-Squared Test, International Statistical Review 51 (1983) 59–72.

[40] H. W. Lilliefors, On the Kolmogorov-Smirnov Test for Normality with Mean and Variance Unknown, Journal of the American Statistical Association 62 (1967) 399–402.

[41] S.-K. Au, J. L. Beck, Estimation of small failure probabilities in high dimensions by subset simulation, Probabilistic Engineering Mechanics 16 (2001) 263–277.

[42] L. L. Zhang, J. Zhang, L. M. Zhang, W. H. Tang, Back analysis of slope failure with Markov chain Monte Carlo simulation, Computers and Geotechnics 37 (2010) 905–912.

[43] T. Alm, L. Hamre, Soil model for pile driveability predictions based on CPT interpretations, in: Proceedings of the 15th International Conference on Soil Mechanics and Geotechnical Engineering, Balkema, Istanbul, Turkey, 2001, pp. 1297–1302.

Appendix A. Notations

B_{stat}	Bartlett statistical value	R_i	Inner skirt resistance
D	Diameter	R_o	Outer skirt resistance
D_i	Inner diameter	R_D	Relative density
D_o	Outer diameter	$R(\tau)$	Theoretical autocorrelation function
f_s	Shaft friction (CPT)	s	Pressure differential
F_r	Normalized shaft friction	s_r	Required suction/underpressure
G	Limit state	s_c	Critical suction
h	Penetration depth	S	Solicitation
i	Exit hydraulic gradient	t	Wall thickness
I_c	Soil behaviour type index	V'	Submerged weight on bucket
k	Permeability	z	Depth
k_f	Shaft friction factor	γ	Safety factor
k_p	End-bearing factor	γ'	Effective soil unit weight
k_r	Permeability ratio	γ_w	Volumetric weight water
K	Stress ratio	δ	Interface friction angle
l_s	Seepage length	δ_v	Vertical scale of fluctuation
L	Skirt length	μ	Mean
m_b	Measurements per window	$\rho(\tau_j)$	Empirical autocorrelation function
N_q	Bearing capacity constant	σ	Standard deviation
N_γ	Bearing capacity constant	σ_v'	Vertical effective stress
q_c	Cone resistance	σ_{vi}'	Inner vertical effective stress
q_t	Corrected cone resistance	σ_{vo}'	Outer vertical effective stress
Q_t	Normalized cone resistance	τ	Separation distance
R	Resistance	ϕ	Angle of internal friction
R_b	End-bearing resistance		

Appendix B. Pseudocode

Appendix B.1. Adapted installation design method for layered soils

Algorithm 1 can be used in combination with CPT-based design [21] as well as the Houlsby & Byrne method [16] (Section 2).

Data: Soil parameters for identified layers at each depth

Result: Required underpressure and critical suction

for *every penetration depth* **do**

    Compute total soil resistance;

    if *total soil resistance ≥ effective submerged weight* **then**

        Save self weight penetration depth;

end

for *every penetration depth ≥ self weight penetration depth* **do**

    Perform seepage analysis;

    Determine critical suction;

    Compute change in soil resistance by applied underpressure

     according to effective stress reduction;

    while *reduced soil resistance ≤ driving forces* **do**

       Raise or lower applied underpressure

    end

    if *required underpressure ≤ critical suction* **then**

        Further suction-assisted penetration feasible;

    else

        Premature refusal;

end

Algorithm 1: Installation design for layered soils of varying permeability

Appendix B.2. Parameter estimation vertical random field cone resistance

Reference is made to [32], [29], [30] for generating the random fields.

Data: Multiple CPTs within one survey dataset

Result: Parameters estimation for a random field model of the cone
resistance for one (CPT) location in the survey data set

for *every CPT in dataset* **do**

Compute soil behavior type index (I_c);

Compute moving window methods;

Find closest borehole log;

Manually identify soil layers;

Verification with second moment Robertson chart

end

for *every layer at location* **do**

Determine trendline and standard deviation;

Compute empirical autocorrelation function;

for *every layer in every other CPT* **do**

if *layers overlap in depth* **then**

else if *layers from same geological deposit* **then**

else if ΔI_c *between layers* $\leq$ *5%* **then**

Add empirical autocorrelation function;

end

Average all added empirical autocorrelation functions;

Fit theoretical autocorrelation models and scale of fluctuation;

end

Algorithm 2: Parameter estimation vertical random fields cone resistance

Appendix B.3. Monte-Carlo simulation

Data: Identified soil layers, random field parameters for cone
      resistance profile simulation (Appendix B.2), probability
      density functions soil parameters, suction bucket dimensions

Result: Probability of failure, 95% reliability intervals

Determine geometric parameters;

Determine amount of iterations (N);

for *every iteration* **do**

    for *every identified layer at the location* **do**

        Simulate random field of the cone resistance;

        Simulate soil parameters from probability density functions;

    end

    Perform adapted installation design method(s) (Appendix B.1);

    Save required underpressure and critical suction profile;

    Normalize limit state with respect to critical suction;

    if *Limit state ≤ 0* **then**

        Failure observed ($N_f + 1$);

end

Compute probability of failure (N_f/N);

for *every depth* **do**

    Determine empirical cumulative density function required and
      underpressure and critical suction;

    Determine 95% reliability intervals from empirical cumulative
      density function;

end